



# Experimental Implementation of a Nonlinear Dynamic Inversion Controller with Antiwindup

Prathyush P. Menon\*

*University of Exeter, Exeter, England EX4 4QF, United Kingdom*

Mark Lowenberg† and Guido Herrmann‡

*University of Bristol, Bristol, England BS8 1TR, United Kingdom*

Matthew C. Turner§

*University of Leicester, Leicester, England LE1 7RH, United Kingdom*

Declan G. Bates¶

*University of Exeter, Exeter, England EX4 4QF, United Kingdom*

and

Ian Postlethwaite\*\*

*Northumbria University, Newcastle upon Tyne, England NE1 8ST, United Kingdom*

DOI: 10.2514/1.59027

A recently proposed nonlinear antiwindup compensation scheme is implemented and tested on a  $\frac{1}{16}$  scaled BAe Hawk jet trainer wind-tunnel model, mounted in a one degree of freedom configuration. The Hawk is modeled as a nonlinear affine system subject to input amplitude constraints. The primary control system consists of an inner-loop nonlinear dynamic inversion controller and an outer-loop linear proportional integral derivative controller. The input constraints are addressed by supplementing this nominal controller with two types of nonlinear antiwindup schemes: a nonlinear variant of the well-known internal model control scheme and a suboptimal  $\mathcal{L}_2$  norm-based antiwindup compensator. Wind tunnel results are presented which demonstrate the usefulness of the antiwindup schemes in preventing performance deterioration due to the input constraints and the flexibility of the proposed approach from a practical perspective.

## Nomenclature

|                  |  |
|------------------|--|
| $A, B, C, D$     | = Plant state space matrices                             |
| $d$              | = disturbance signal                                     |
| $Dz$             | = deadzone operator                                      |
| $M_\theta, M_q,$ | = pitching moment derivatives with regard to $\theta, q$ |
| $M_\eta$         |  |
| $q$              | = pitch rate, deg /s                                     |
| $Re$             | = Reynolds number  |
| $r$              | = reference signal                                       |
| $\text{sat}$     | = saturation operator                                    |
| $u$              | = control input vector                                   |
| $x$              | = state vector   |
| $y$              | = measurement vector                                     |
| $z$              | = performance output vector                              |
| $\eta$           | = tailplane deflection, deg                              |
| $\theta$         | = pitch angle, deg                                       |
| $\mathcal{L}_2$  | = Lebesgue space of square integrable functions          |
| $\mathbb{R}$     | = field of real numbers                                  |
| $s$              | = Laplace variable                                       |

## Subscripts

|                  |  |
|------------------|--|
| aw, c, lin       | = antiwindup, control, and linear signal identifiers           |
| nom, pd,         | = nominal, plant disturbance, and saturated signal identifiers |
| sat              |  |
| max              | = maximum  |
| min              | = minimum  |
| $\lambda_{\min}$ | = smallest eigenvalue of a matrix                              |

## I. Introduction

NONLINEAR dynamic inversion is a promising approach for direct nonlinear control system design and has attracted significant attention from the aerospace community [1–13]. The nonlinear dynamic inversion (NDI) approach works effectively, by using nonlinear state feedback to cancel the plant's nonlinear terms, and then standard linear control techniques to provide desirable closed-loop performance properties. In principle, the designer must have perfect knowledge of the system dynamics and the controller should have access to the plant state vector. Although in practice such assumptions are not entirely realistic, there remains much interest in NDI due to the elegant simplicity of the approach; moreover, various studies appear to suggest that NDI controllers can work well in real systems, despite concerns over robustness.

The NDI approach was developed, however, without explicit consideration of control signal constraints, which are inevitably present in all physical actuators. It is well known from the study of constrained linear systems that systems which are otherwise well designed can exhibit dramatic changes in their stability and performance properties in the event of actuator saturation. Thus, in a flight-control context, aggressive high pilot gain maneuvering may lead to actuator saturation and an ensuing loss of performance and/or stability. Because of the plant inversion taking place, NDI controllers may be equally, and potentially more, susceptible to saturation problems compared to their linear counterparts.

Presented as Paper 2008-6791 at the AIAA Guidance, Navigation and Control Conference and Exhibit, Honolulu, HI, 18–21 August 2008; received 21 May 2012; revision received 7 October 2012; accepted for publication 17 October 2012; published online 6 May 2013. Copyright © 2012 by the American Institute of Aeronautics and Astronautics, Inc. All rights reserved. Copies of this paper may be made for personal or internal use, on condition that the copier pay the \$10.00 per-copy fee to the Copyright Clearance Center, Inc., 222 Rosewood Drive, Danvers, MA 01923; include the code 1533-3884/13 and \$10.00 in correspondence with the CCC.

\*Lecturer, College of Engineering Mathematics and Physical Sciences.

†Reader, Department of Aerospace Engineering. Senior Member AIAA.

‡Reader, Department of Mechanical Engineering.

§Senior Lecturer, Department of Engineering.

¶Professor, College of Engineering Mathematics and Physical Science.

\*\*Deputy Vice-Chancellor.

Linear systems subject to control constraints have been studied for many years and various methods for handling these constraints have been proposed. One approach that has found favor in industry and academia is the so-called antiwindup (AW) approach: first a linear controller is designed in ignorance of saturation constraints; then an AW compensator is designed with the sole purpose of assisting the linear controller during and after a saturation event. Antiwindup design has been studied extensively in the context of linear systems with earlier work [14–17] seeking to provide useful practical solutions to the problem and then complemented by theoretical studies, which looked at the existence of particular solutions of AW compensators. For instance, the existence of AW compensators was studied, which guarantees global exponential stability [18–20], although a nominal controller was designed without the actuator saturation in mind; the necessary and sufficient condition is an open-loop exponentially stable system. Later work contributed systematic synthesis routines with stability/performance guarantees of various types [21–27]. Even open-loop stable systems may exhibit dramatic performance and stability deterioration during actuator saturation and the design of AW compensators is challenging and practically significant [28]. More detail on existing approaches to AW can be found in recent books [29,30] and surveys [31,32].

Although AW schemes for linear systems are plentiful (e.g., recent work by [13] for a linear dynamic inversion control problem), they are scarce for nonlinear systems. At least part of the reason for this is the generality of this class of systems, which makes the problem more complex. Another reason is that the computation associated with nonlinear AW design is typically rather difficult. Investigation of nonlinear AW techniques has begun to appear in the literature and we refer the reader to [33] for an adaptive AW scheme and [34] for a convergence-based AW scheme. Work on nonlinear Euler–Lagrange systems may also be found in [29]. It appears that consideration of special classes of system is useful, if not vital, in AW design for nonlinear systems.

Recently a nonlinear AW scheme has been proposed which generalized key ideas of linear AW to a certain class of nonlinear systems under NDI control [35]. The scheme extends the work of [18,36–38] to the NDI setting and, in particular, generalizes the coprime factorisation approaches of the linear scheme to the nonlinear case. Hence, the scheme of [35] contains results which in principle allow one to design globally stabilising AW compensators, which lead to minimal  $\mathcal{L}_2$  performance deterioration, providing the plant is globally exponentially stable. The nonlinear internal model control (IMC) AW compensator appears as a special case and in [35] an optimization procedure was suggested for the design of optimal AW compensators. This optimization problem is the nonlinear counterpart of the linear matrix inequality (LMI) optimization problem found in the linear setting [24,38] but is generally nonconvex in nature and robust nonlinear optimization methods are necessary.

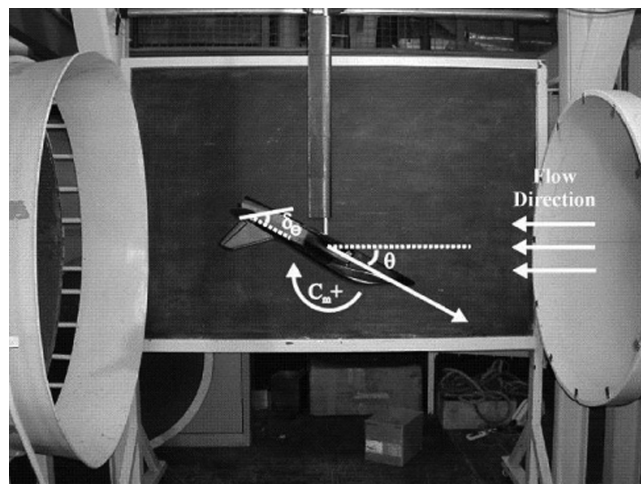


Fig. 1 The wind-tunnel rig in the University of Bristol 1.1 m openjet tunnel.

**Table 1 Physical characteristics of the 1/16th scale BAe Hawk model**

| Characteristic                | Value                       |
|-------------------------------|-----------------------------|
| Length                        | 0.655 m                     |
| Wing span                     | 0.612 m                     |
| Mean aerodynamic chord        | 0.135 m                     |
| Mass                          | 1.8 kg                      |
| Inertia about x-axis $I_{xx}$ | 0.00959 kg · m <sup>2</sup> |
| Inertia about y-axis $I_{yy}$ | 0.0395 kg · m <sup>2</sup>  |
| Inertia about z-axis $I_{zz}$ | 0.0507 kg · m <sup>2</sup>  |

The main contribution of the current paper is the application of the nonlinear AW theory described above to a realistic aerospace experimental setup. Although some experimental AW work has been reported recently [28,39–41], these references mainly concentrate on linear AW approaches. Because the significance of NDI control in the aerospace community, the aim of this paper is to present the application of the NDI AW approach developed in [35] to an experimental aerospace system, namely, an approximate BAe Hawk scale model. Although the Hawk model considered here does not satisfy all the assumptions given in [35], it is shown how those results may be applied in a local manner, allowing the NDI AW compensator to guarantee local performance and  $\mathcal{L}_2$  gain properties. Results of wind-tunnel testing show that, in the presence of control constraints, the system equipped with the NDI AW compensator yields superior performance to that without it.

## II. Wind-Tunnel Model

The wind-tunnel model used in the rig is an approximate  $\frac{1}{16}$ th scale BAe Hawk, a trainer aircraft, as shown in Fig. 1. The physical characteristics of the model, referred to hereafter simply as the Hawk, are provided in Table 1. For the experimental setup, the model may only rotate about its lateral axis. Only angular position  $\theta$  is measured, using a precision carbon-film potentiometer, accurate up to  $\pm 0.05$  deg. The tailplane deflection controls the pitch. The left and right tailplanes are directly driven by miniature model aircraft servos such that their deflections are always the same, i.e., as if there were a single-piece tailplane; we subsequently refer only to a single tailplane deflection angle. A dSPACE DS1103 real-time control system workstation<sup>††</sup> is employed for data acquisition and control, using Matlab/Simulink and Real-Time Workshop for rapid control system prototyping. The sampling rate used is 100 Hz. The wind tunnel used for experiments is a 1.1-m-diam openjet tunnel with a maximum speed of 40 m/s, and a turbulence level of approximately 1.5% at 20 m/s, which generates a significant level of disturbance to the system. All experiments are performed at 20 m/s corresponding to  $Re = 0.2 \times 10^6$  based on model wing chord.

The flow velocity is assumed to be exactly horizontal in the tunnel working section, so that the set up represents level trim flight conditions, i.e., where angle of attack  $\alpha$  is the same as the pitch angle  $\theta$ . For controller design, an approximate numerical model of the model installed on the wind-tunnel rig, developed in [42], is used. The numerical model captures the nonlinear dynamics of the wind-tunnel model, including the fixed point equilibrium solutions, the Hopf bifurcations, and limit cycle oscillations. The present study is limited to the low- $\alpha$  stable branch of the model. Previous experimental control studies on the Hawk in this wind tunnel include different proportional integral derivative (PID) controllers [43] and a nonlinear dynamic gain scheduled controller [44].

The pitch acceleration is represented as a function of the pitch angle, pitch rate, and the tailplane deflection

$$\ddot{\theta} = M_q(\theta, \dot{\theta}, \eta)q + M_\theta(\theta, \dot{\theta}, \eta)\theta + M_\eta(\theta, \dot{\theta}, \eta)\eta$$

<sup>††</sup>dSPACE is a registered trademark of dSPACE GmbH. Data available online at <http://www.dspace.com/en/inc/home/products/hw/singbord/ppcconbo.cfm>.

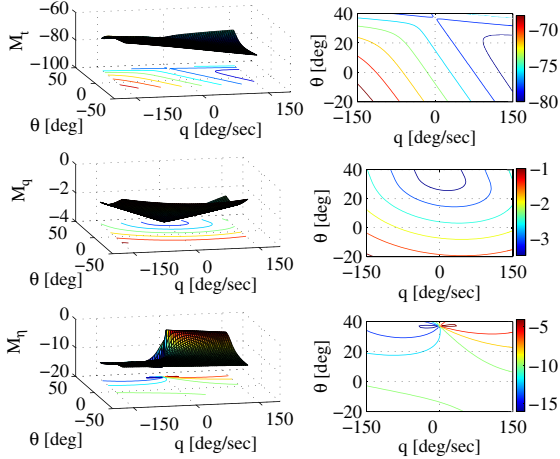


**Fig. 2** Nonlinear parameter dependent coefficients for  $\eta = 4$  deg.

where  $M_q$ ,  $M_\theta$  and  $M_\eta$  are nonlinear parameter dependent coefficients. Hence, this nonlinear model can be represented as an optimized three-dimensional look-up table, so that  $M_q$ ,  $M_\theta$ , and  $M_\eta$  are computed a priori for all possible combinations of the independent variables  $\theta$ ,  $\dot{\theta}$ , and  $\eta$ , and stored in a multidimensional look-up table.  $M_q$ ,  $M_\theta$ , and  $M_\eta$  are dependent strongly on  $\theta$  and  $q$ , but have negligible dependence on  $\eta$  near the trim point  $\tilde{\eta} = 4$  deg. The nonlinearities in model mainly arise from the parameter dependent coefficients. The interval of interest for the tailplane deflection  $\eta$  is chosen to be  $[-3.75 \text{ deg}, 4.75 \text{ deg}]$ . In this interval, the practical Hawk wind-tunnel model and its simulation model are stable and the dependency on  $\eta$  is not as strong as for the unstable operating region of the Hawk. The considered region corresponds to the usual piloting region of the BAe Hawk trainer aircraft in level flight cruise conditions, also considering the correct actuator range in [45]. The parameter dependent coefficients have strong dependency on pitch  $\theta$  and pitch rate  $\dot{\theta}$  in contrast to the tailplane deflection  $\eta$  which proves to have very little influence. The considered plant and model is highly nonlinear, resembling a quasi-linear parameter varying system [43,45]. This ideally suits the AW approach to be presented in this paper. For NDI control and NDI AW design a good approximate model is:

$$\begin{bmatrix} \dot{q} \\ \dot{\theta} \end{bmatrix} = \begin{bmatrix} M_q(\theta, \dot{\theta}, \tilde{\eta})|_{\tilde{\eta}=4} & M_\theta(\theta, \dot{\theta}, \tilde{\eta})|_{\tilde{\eta}=4} \\ 1 & 0 \end{bmatrix} \begin{bmatrix} q \\ \theta \end{bmatrix} + \begin{bmatrix} M_\eta(\theta, \dot{\theta}, \tilde{\eta})|_{\tilde{\eta}=4} \\ 0 \end{bmatrix} \eta \quad (1)$$

The nonlinear behavior of the coefficients is shown in Fig. 2. The left subplots in Fig. 2 provide the surface plots of  $M_\theta$ ,  $M_q$ , and  $M_\eta$  as functions of the pitch angle  $\theta$  and the pitch velocity  $q$ , while the third parameter  $\eta$  is fixed at 4 deg, the level trim condition. The model still reflects all major nonlinearities of the Hawk for the considered operating region.

The variable  $\eta$  is not measured in the experimental setup and for the purpose of designing the controller and compensators, a second-order actuator model is employed to represent the dynamics of the servo motor driven actuator. The actuator transfer function (see [45] for details on the actuator modeling) is:

$$\frac{\eta}{\eta_{\text{demand}}} = \frac{5 \times 10^4}{s^2 + 1250s + 5 \times 10^4}$$

### III. Background Theory for Design of AW Compensators

#### A. Notation

Standard notation is followed throughout the paper. The following identity relates the saturation and deadzone functions

$$\text{sat}(u) = u - \text{Dz}(u) \quad (2)$$

$$\text{sat}(u) = \begin{bmatrix} \text{sat}_1(u_1) \\ \vdots \\ \text{sat}_m(u_m) \end{bmatrix}, \quad \text{Dz}(u) = \begin{bmatrix} \text{Dz}_1(u_1) \\ \vdots \\ \text{Dz}_m(u_m) \end{bmatrix} \quad (3)$$

where  $u \in \mathbb{R}^m$  and  $\text{sat}_i(u_i) = \text{sign}(u_i) \min(|u_i|, \bar{u}_i)$ ,  $\forall i$  and  $\text{Dz}_i(u_i) = \text{sign}(u_i) \max(0, |u_i| - \bar{u}_i)$ ,  $\forall i$  and the limits  $\bar{u}_i > 0$ ,  $\forall i \in \{1, \dots, m\}$ . It follows from the graphs of these functions that for some positive definite diagonal matrix  $W > 0$ , the following inequality holds

$$\tilde{u}' W (\tilde{u} - \tilde{u}) \geq 0 \quad (4)$$

where  $\tilde{u} = \text{Dz}(u)$ , or  $\tilde{u} = \text{sat}(u)$ . The  $\mathcal{L}_2$  norm of a signal is defined as

$$\|x\|_2 = \sqrt{\int_0^\infty \|x\|^2 dt}$$

and the induces  $\mathcal{L}_2$  norm, or  $\mathcal{L}_2$  gain, for nonlinear operator,  $\mathcal{H}$ , is defined as

$$\|\mathcal{H}\|_{i,2} := \sup_{0 \neq x \in \mathcal{L}_2} \frac{\|\mathcal{H}x\|_2}{\|x\|_2}$$

#### B. System Definition and Assumptions

This section introduces a recently proposed NDI AW strategy on which the main results of this paper, an experimental implementation of a nonlinear AW scheme, are based. Thus, for this purpose, a class of nonlinear affine systems is considered

$$\dot{x} = Ax + B[f(x) + G(x)u_m] + B_{pd}d \quad (5)$$

$$y = Cx + D_{pd}d \quad (6)$$

where  $x \in \mathbb{R}^n$  is the state vector of the system;  $u_m := \text{sat}(u) \in \mathbb{R}^m$  is the input to the plant,  $u \in \mathbb{R}^m$  is the controller output (implying the existence of a saturation block, often introduced artificially to respect the hard constraints, between the controller and the actual plant), and  $y \in \mathbb{R}^p$  is the output vector. The  $A$ ,  $B$ ,  $B_{pd}$ ,  $C$ , and  $D_{pd}$  matrices are of appropriate dimensions. The bounded exogenous disturbance signal is represented as  $d \in \mathbb{R}^{n_d}$ . It is assumed throughout that  $f(x)$  is Lipschitz and that the matrix  $G(x)$  is invertible for all  $x \in \mathbb{R}^n$ . For feedback control design, it is assumed that the entire state  $x$  is available. The range space of the nonlinear part of the model is assumed to be a subspace of the range space of our control input.

As reported in [18,46], a common assumption in AW compensator design is open-loop exponential stability of the plant under consideration; that is when  $u_m = 0$  and  $d = 0$ , the origin of  $\dot{x} = Ax + Bf(x)$  is exponentially stable. Such an assumption is necessary only when global exponential stability of the saturated closed-loop system is sought. This may also motivate our choice of plant investigated. However, in this paper, only *local exponential* stability is required and hence, the results developed in [35] to ensure global stability are modified to fit the arguments in the *local* sense.

The linear part of the NDI control scheme is given by

$$K \sim \begin{cases} \dot{x}_c = A_c x_c + B_c y + B_{cr} r \\ u_{lin} = C_c x_c + D_c y + D_{cr} r \end{cases} \quad (7)$$

where  $x_c \in \mathbb{R}^{n_c}$  is the linear controller state,  $r \in \mathbb{R}^{n_r} \cap \mathcal{L}_p$  represents the disturbance on the controller, normally the reference input, and  $u_{lin} \in \mathbb{R}^m$  is the output of the linear controller. The matrices  $A_c$ ,  $B_c$ ,  $C_c$ ,  $D_c$ ,  $B_{cr}$ , and  $D_{cr}$  are the controller system matrices of appropriate dimensions. We assume that, under the control law,

$$u = \underbrace{G(x)^{-1}[-f(x) + u_{\text{lin}}]}_{u_{\text{nom}}} \quad (8)$$

the closed-loop system given by Eqs. (5) and (8) is well-posed and the origin is exponentially stable in a well defined compact set around the origin, i.e., the operating region of the nominal controller designed without consideration of the actuator saturation. This is a common but important assumption, characterizing the *nominal* (i.e., unsaturated) behavior of the system. It is assumed that  $\|G(x)^{-1}\|$  is bounded for all  $x$  in some compact set to be defined later.

### C. Constrained Nonlinear Closed-Loop System Description

The assumption on  $\|G(x)^{-1}\|$  guarantees a nonsingular matrix  $G(x)$  for all  $x \in \mathbb{R}^n$ , or at least in the considered local compact set for all the time. However, this assumption of nonsingularity may not prevent extreme cases. For instance, in some portions of the system's state space,  $G(x)$  may be nonsingular, but may be almost singular, meaning that  $G(x)^{-1}$  will, in a certain sense, be large and hence by Eq. (8), the control input may have a very large magnitude. Obviously in practice, the control signal will saturate for sufficiently large values of demanded control. It is also important that the system tracks the reference well even in the presence of input constraints.

In the presence of input saturation, the closed-loop system satisfies  $u_m = \text{sat}(u)$  and hence, the system's state equation is:

$$\dot{x} = Ax + B[f(x) + G(x)\text{sat}(u)] + B_{\text{pd}}d \quad (9)$$

To limit the degradation of the tracking performance while saturation occurs, an AW compensator is introduced as

$$\dot{x}_{\text{aw}} = Ax_{\text{aw}} + B[f(x_{\text{aw}}) + G(x)(h(x_{\text{aw}}) - Dz(u))], \quad x_{\text{aw}}(t=0) \quad (10)$$

$$\theta_1 = h(x_{\text{aw}}) + G(x)^{-1}f(x_{\text{aw}}), \quad \theta_2 = Cx_{\text{aw}} \quad (11)$$

where  $x_{\text{aw}} \in \mathbb{R}^n$  and  $\theta_1 \in \mathbb{R}^n$  and  $\theta_2 \in \mathbb{R}^p$ . The matrices and functions  $A$ ,  $B$ ,  $C$ ,  $f(\cdot)$ ,  $G(\cdot)$  and  $h(\cdot)$  are inherited from the plant description (5) and (6). Note that the initial condition of the AW compensator is usually  $x_{\text{aw}}(t=0)$ , which guarantees that  $x_{\text{aw}}(t=0)$  is within an invariant set, introduced later, and the AW compensator is inactive should the initial control  $u(t=0)$  be within the saturation limits. However, this is a practical consideration and not a necessity. The AW compensator modifies the control input to the system to be

$$u = G(x)^{-1}[-f(x) + u_{\text{lin}}] + \theta_1 \quad (12)$$

where  $u_{\text{lin}}$  is modified from that of the  $u_{\text{nom}}$  structure shown in Eqs. (7) and (8), with the linear AW compensation signal  $\theta_2$  as follows:

$$K \sim \begin{cases} \dot{x}_c = A_c x_c + B_c(y - \theta_2) + B_{\text{cr}}r \\ u_{\text{lin}} = C_c x_c + D_c(y - \theta_2) + D_{\text{cr}}r \end{cases} \quad (13)$$

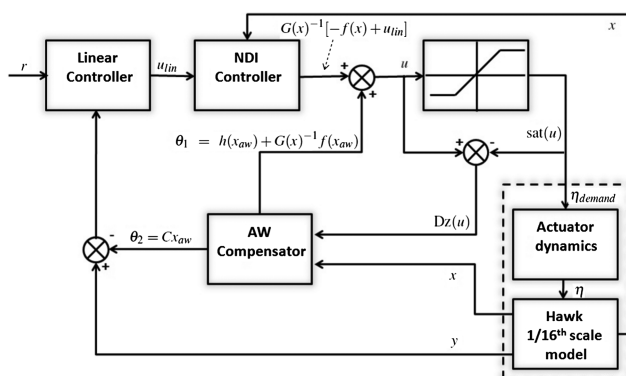


**Fig. 3** The closed-loop plant with antiwindup block schematic diagram ( $d = 0$ ).

The architecture of the closed-loop system with AW compensator is as shown in Fig. 3. The form of this compensator is essentially an NDI version of the compensator used in [24,36,37]; it basically consists of a copy of the nominal plant, driven by the deadzone function and augmented with extra feedbacks  $\theta_1$  and  $\theta_2$  to improve the system's behavior and tracking performance while saturation is active. The free parameter function  $h(\cdot)$  will be chosen so that stability of the AW scheme is achieved and performance close to nominal control is recovered. A simple requirement for  $h(\cdot)$  is that when  $Dz(u) = 0$  (i.e., when saturation does not occur), the system

$$\dot{x}_{\text{aw}} = Ax_{\text{aw}} + B[f(x_{\text{aw}}) + G(x)h(x_{\text{aw}})] \quad (14)$$

has to be (locally) exponentially stable. By the assumption on the stability of the plant, such a function always exists,  $h(x_{\text{aw}}) = 0$ , and is shown to correspond to the IMC AW solution in sequel. Note that in the formulation of Eqs. (10) and (11), an additional state feedback from the nominal system, due to the presence of the  $G(x)$  term, is required in the AW compensator.

### D. IMC Approach for AW Compensation

A well known AW technique is that of IMC [35,47], which essentially consists of a copy of the plant for AW compensator synthesis. The IMC AW compensator is obtained by setting the term  $h(x_{\text{aw}}) \equiv 0$  in Eqs. (10) and (11), which further yields

$$\dot{x}_{\text{aw}} = Ax_{\text{aw}} + B[f(x_{\text{aw}}) - G(x)Dz(u)] \quad (15)$$

$$\theta_1 = G(x)^{-1}f(x_{\text{aw}}), \quad \theta_2 = Cx_{\text{aw}} \quad (16)$$

and is similar to the linear scheme as in [47]. The following theorem shows that this is also the case for the class of nonlinear systems which we consider.

*Theorem 1:* The origin of the closed-loop system consisting of the system in Eq. (9), the control law in Eq. (12), and the IMC AW compensator (15) and (16)  $h(x_{\text{aw}}) := 0$ , is locally exponentially stable. The original invariant set of the nominal closed-loop system is recovered:

*Proof:* First note that using the identity (2), the state equation can be rewritten as:

$$\begin{aligned} \dot{x} &= Ax + B[f(x_{\text{aw}}) + C_c x_c + D_c(y - \theta_2) \\ &\quad + D_{\text{cr}}r - G(x)Dz(u)] + B_{\text{pd}}d \end{aligned} \quad (17)$$

In a similar manner to [48], define the error signal  $e(t) := x(t) - x_{\text{aw}}(t)$ . From this, it follows that:

$$\dot{e} = (A + BD_c C)e + BC_c x_c + BD_{\text{cr}}r + (B_{\text{pd}} + BD_c D_{\text{pd}})d \quad (18)$$

$$\dot{x}_c = A_c x_c + B_c Ce + B_{\text{cr}}r + B_c D_{\text{pd}}d \quad (19)$$

Rearranging Eqs. (18) and (19) in the matrix form yields

$$\begin{bmatrix} \dot{e} \\ \dot{x}_c \end{bmatrix} = \underbrace{\begin{bmatrix} (A + BD_c C) & BC_c \\ B_c C & A_c \end{bmatrix}}_{A_{\text{lin}}} \begin{bmatrix} e \\ x_c \end{bmatrix} + \underbrace{\begin{bmatrix} BD_{\text{cr}} & (B_{\text{pd}} + BD_c D_{\text{pd}}) \\ B_{\text{cr}} & B_c D_{\text{pd}} \end{bmatrix}}_{B_{\text{lin}}} \begin{bmatrix} r \\ d \end{bmatrix} \quad (20)$$

where  $A_{\text{lin}}$  and  $B_{\text{lin}}$  represent the nominal closed-loop and input distribution matrices respectively, i.e.,  $A_{\text{lin}}$  is Hurwitz by design.

Defining  $[e \sim x_c]^T = X_{\text{lin}}$  and  $[r \sim d]^T = \hat{W}$ , Eq. (20) is rewritten as:

$$\dot{X}_{\text{lin}} = A_{\text{lin}} X_{\text{lin}} + B_{\text{lin}} \hat{W} \quad (21)$$

Note the linear stable character of the dynamics of  $X_{\text{lin}}$  in Eq. (20) fully determined by the nominal closed loop, i.e., a bounded  $\hat{W}$ , will result also in a bounded state  $X_{\text{lin}}$ . Thus, there exists  $P_{\text{lin}} > 0$  so that  $P_{\text{lin}}A_{\text{lin}} + A_{\text{lin}}P = -I$ . Hence,  $V_{\text{lin}} = X_{\text{lin}}^T P_{\text{lin}} X_{\text{lin}}$  can be defined. Thus,

$$\begin{aligned}\dot{V}_{\text{lin}} &= -X_{\text{lin}}^T X_{\text{lin}} + 2X_{\text{lin}}^T P_{\text{lin}} B_{\text{lin}} \hat{W} \\ &\leq -X_{\text{lin}}^T X_{\text{lin}} + 2\|X_{\text{lin}}\| \|P_{\text{lin}} B_{\text{lin}}\| \|\hat{W}\| \\ &\leq -X_{\text{lin}}^T X_{\text{lin}} + \|X_{\text{lin}}\|^2 \frac{\|P_{\text{lin}} B_{\text{lin}}\|^2}{\varepsilon_{\text{lin}}} + \varepsilon_{\text{lin}} \|\hat{W}\|^2\end{aligned}\quad (22)$$

for some scalar  $\varepsilon_{\text{lin}} > 0$ . This implies for large enough  $\varepsilon_{\text{lin}} > 0$  that

$$\dot{V}_{\text{lin}} \leq -0.5X_{\text{lin}}^T X_{\text{lin}} + \varepsilon_{\text{lin}} \hat{W}^T \hat{W}$$

The Lyapunov function  $V_{\text{lin}}$  will be considered for the analysis of the overall closed-loop system.

To complete the whole closed-loop system analysis, we can rewrite Eq. (15) as:

$$\begin{aligned}\dot{x}_{\text{aw}} &= Ax_{\text{aw}} + Bf(x_{\text{aw}}) + BDz[G(x)^{-1}(f(x) \\ &\quad - f(x_{\text{aw}}) - D_c Ce - C_c x_c - D_{\text{cr}} r - D_c D_{\text{pd}} d)]\end{aligned}\quad (23)$$

The open-loop system is (locally) exponentially stable; thus for some positive definite function  $V(x_{\text{aw}})$ , there exist by the converse Lyapunov theorem ([49] Theorem 4.14, pp. 162–163) the constants,  $\alpha_i$ ,  $i = 1, \dots, 4$ , such that

$$\alpha_1 \|x_{\text{aw}}\|^2 \leq V(x_{\text{aw}}) \leq \alpha_2 \|x_{\text{aw}}\|^2 \quad (24)$$

$$\frac{\partial V(x_{\text{aw}})}{\partial x_{\text{aw}}} [Ax_{\text{aw}} + Bf(x_{\text{aw}})] \leq -\alpha_4 \|x_{\text{aw}}\|^2 \quad (25)$$

$$\left\| \frac{\partial V(x_{\text{aw}})}{\partial x_{\text{aw}}} \right\| \leq \alpha_3 \|x_{\text{aw}}\| \quad (26)$$

for all  $x_{\text{aw}} \in \mathcal{C}$  where  $\mathcal{C}$  is a compact set containing the origin in its interior. The compact set  $\mathcal{C}$  is a subset of the invariant set defined by the nominal controller. Thus, we obtain for  $x_{\text{aw}} \in \mathcal{C}$

$$\begin{aligned}\dot{V}(x_{\text{aw}}) &\leq -\alpha_4 \|x_{\text{aw}}\|^2 + \alpha_3 \|B\| \|x_{\text{aw}}\| \|Dz(u)\| \\ &\leq -\alpha_4 \|x_{\text{aw}}\|^2 + \alpha_3 \|x_{\text{aw}}\| \|B\| \|G(x)^{-1}\| \|f(x) \\ &\quad - f(x_{\text{aw}}) - C_c x_c - D_c Ce - D_{\text{cr}} r\|\end{aligned}\quad (27)$$

Lipschitz continuity of  $f(\cdot)$  implies that  $\|f(x) - f(x_{\text{aw}})\| \leq K_1 \|x - x_{\text{aw}}\| = K_1 \|e\| K_1 \|x - x_{\text{aw}}\| = K_1 \|e\|$ . Equation (27) thus becomes:

$$\begin{aligned}\dot{V}(x_{\text{aw}}) &\leq -\alpha_4 \|x_{\text{aw}}\|^2 \\ &\quad + \alpha_3 \|B\| \|G(x)^{-1}\| \|x_{\text{aw}}\| [K_1 + \|[-D_c C \quad -C_c]\|] \|X_{\text{lin}}\| \\ &\quad + \alpha_3 \|B\| \|G(x)^{-1}\| \|x_{\text{aw}}\| \|[D_{\text{cr}} \quad D_c D_{\text{pd}}]\| \|\hat{W}\|\end{aligned}\quad (28)$$

Introducing scalars  $k_1 > 0$  and  $k_2 > 0$  we such that

$$\begin{aligned}k_1 &\geq \frac{1}{2} \alpha_3 \|B\| \|G(x)^{-1}\| [K_1 + \|[-D_c C \quad -C_c]\|], \\ k_2 &\geq \frac{1}{2} \alpha_3 \|B\| \|G(x)^{-1}\| \|[D_{\text{cr}} \quad D_c D_{\text{pd}}]\|\end{aligned}$$

Equation (28) is rewritten as:

$$\dot{V}(x_{\text{aw}}) \leq -\alpha_4 \|x_{\text{aw}}\|^2 + 2\|x_{\text{aw}}\| [k_1 \|X_{\text{lin}}\| + k_2 \|\hat{W}\|] \quad (29)$$

Applying Young's inequality  $2\varepsilon a^T \frac{b}{\varepsilon} \leq \varepsilon^2 \|a\|^2 + \frac{\|b\|^2}{\varepsilon^2}$ , for all  $\varepsilon > 0$ , Eq. (29) is rewritten as

$$\begin{aligned}\dot{V}(x_{\text{aw}}) &\leq -\alpha_5 \|x_{\text{aw}}\|^2 + \frac{k_1^2}{\varepsilon_1^2} \|X_{\text{lin}}\|^2 + \frac{k_2^2}{\varepsilon_2^2} \|\hat{W}\|^2, \\ &\leq -\frac{\alpha_5}{\alpha_2} V(x_{\text{aw}}) + \frac{k_1^2}{\varepsilon_1^2} \|X_{\text{lin}}\|^2 + \frac{k_2^2}{\varepsilon_2^2} \|\hat{W}\|^2, \quad x_{\text{aw}} \in \mathcal{C}\end{aligned}\quad (30)$$

for which the constants  $\varepsilon_1, \varepsilon_2 > 0$  have been chosen small enough so that

$$\alpha_4 \geq \underbrace{(\varepsilon_1^2 k_1^2 + \varepsilon_2^2 k_2^2)}_{\phi}$$

and  $\alpha_5 = \alpha_4 - \phi > 0$ .

Thus, using  $k_l V_{\text{lin}} + V$  as a Lyapunov function ( $k_l > 0$ ) for the whole closed-loop with AW compensation, we have:

$$\begin{aligned}k_l \dot{V}_{\text{lin}} + \dot{V} &\leq -0.5k_l X_{\text{lin}}^T X_{\text{lin}} + k_l \varepsilon_{\text{lin}} \hat{W}^T \hat{W} - \frac{\alpha_5}{\alpha_2} V(x_{\text{aw}}) \\ &\quad + \frac{k_1^2}{\varepsilon_1^2} \|X_{\text{lin}}\|^2 + \frac{k_2^2}{\varepsilon_2^2} \|\hat{W}\|^2\end{aligned}\quad (31)$$

Now the scalar  $k_l > 0$  can be chosen so that  $0.5k_l > (k_1^2/\varepsilon_1^2)$  and there is a  $k_L > 0$  which satisfies:

$$k_L \frac{k_l}{\lambda_{\min}(P_{\text{lin}})} = 0.5k_l - \frac{k_1^2}{\varepsilon_1^2}$$

This implies:

$$\begin{aligned}k_l \dot{V}_{\text{lin}} + \dot{V} &\leq -k_L k_l V_{\text{lin}} - \frac{\alpha_5}{\alpha_2} V(x_{\text{aw}}) + \left\{ k_l \varepsilon_{\text{lin}} + \frac{k_2^2}{\varepsilon_2^2} \right\} \|\hat{W}\|^2 \\ &\leq -\min\left(k_L, \frac{\alpha_5}{\alpha_2}\right) (k_l V_{\text{lin}} + V(x_{\text{aw}})) + \left\{ k_l \varepsilon_{\text{lin}} + \frac{k_2^2}{\varepsilon_2^2} \right\} \|\hat{W}\|^2\end{aligned}\quad (32)$$

For local stability, a small signal argument needs to be made. Hence, the bound  $B_{\hat{W}}$  for  $B_{\hat{W}} \geq \|\hat{W}\|$  needs to be sufficiently small. Provided the set

$$\mathcal{S} = \left\{ (e, x_c, x_{\text{aw}}) | (k_l V_{\text{lin}} - V(x_{\text{aw}})) \leq \left\{ \frac{k_l \varepsilon_{\text{lin}}}{\min(k_L, \frac{\alpha_5}{\alpha_2})} + \frac{k_2^2}{\min(k_L, \frac{\alpha_5}{\alpha_2}) \varepsilon_2^2} \right\} B_{\hat{W}}^2 \right\}$$

is a subset of  $\mathbb{R}^n \times \mathbb{R}^{n_c} \times \mathcal{C}$ , this will guarantee that  $\mathbb{R}^n \times \mathbb{R}^{n_c} \times \mathcal{C}$  is an invariant set. This establishes that the original invariant set of the closed-loop system is recovered for small enough exogenous demand  $r$  and disturbance  $d$ .

The proof of Theorem 1 implies that the closed-loop system with IMC AW will recover the invariant set associated with the nominal (unsaturated) system. One of the attractive properties of the IMC AW techniques is that stability is guaranteed unconditionally for the open-loop stable (non)linear system [35]. Despite its ease of construction and guaranteed stability properties, researchers have found the performance of the IMC AW compensator to be typically quite poor [23], even for linear systems. We cannot expect the situation to improve for nonlinear systems with NDI controllers, and a possible optimization approach providing better performing AW compensators is introduced in [35]. Thus, a constructive approach for performance is presented next.

## E. $\mathcal{L}_2$ Gain Optimization and Optimal NDI AW Design

To improve upon the IMC performance, it is necessary to devise some more appealing way of choosing our free parameter  $h(x_{\text{aw}})$ . As suggested in [35,50], we use an  $\mathcal{L}_2$  optimization framework to synthesize  $h(x_{\text{aw}})$ . In this case, a fictitious input signal  $w \in \mathbb{R}^m$  and a performance output  $z$ , which we assume is linear in the

plant states, are introduced; thus our system under consideration becomes:

$$\dot{x} = Ax + B[f(x) + G(x)(\text{sat}(u) - w)] + B_{pd}d \quad (33)$$

$$y = Cx + D_{pd}d \quad (34)$$

$$z = C_z x \quad (35)$$

The AW compensator described as in Eqs. (10) and (11) is used. However, the control law (8) is augmented to include  $w$ , that is,

$$u = G(x)^{-1}[-f(x) + u_{lin}] + \theta_1 + w \quad (36)$$

where  $u_{lin}$  is the same as given in (13), which is a function of  $\theta_2$  generated by the AW compensator (10) and (11). The scalar  $\mathcal{L}_2$  gain  $\gamma > 0$  ([49] p. 209), given in Eq. (37), is minimized to optimize the performance of the system:

$$\gamma := \sup_{w \neq 0} \frac{\|z\|_2}{\|w\|_2} \quad (37)$$

A similar type of performance index was used in [51] and it was found for linear plants [52] that the  $\mathcal{L}_2$  gain minimization approach attempts to design the AW compensator so that performance of the control system with saturation remains close to that of the nominal closed-loop system. This fact has been used to generalize the optimization approach of [37,38] to a nonlinear setting (see also [35]).

The design of the NDI AW can be summarized in the following theorem and the proof is given here for completeness (a nonlinear extension and equivalence of the proof from a coprime factorization perspective of the well known Weston–Postlethwaite scheme can be seen in [35]):

**Theorem 2:** There exists an AW compensator (10) and (11) which ensures that the origin of the closed-loop system (33–36) (10) and (11) is asymptotically stable when  $w = 0$  and the map  $\mathcal{T}_p: w \mapsto z$  has  $\mathcal{L}_2$  gain less than  $\gamma$  (in a local sense) if there exist functions  $V(x_{aw}) > 0$  and  $h(x_{aw})$ , a diagonal matrix  $W > 0$  and a scalar  $\varepsilon > 0$  such that the following inequality is satisfied for all  $x_{aw} \neq 0$  and  $x$  inside the nominal invariant set:

$$\begin{bmatrix} \frac{\partial V}{\partial x_{aw}}[Ax_{aw} + Bf(x_{aw}) + BG(x)h(x_{aw})] + x'_{aw}C'_z C_z x_{aw} & \frac{1}{2}\left[\frac{\partial V}{\partial x_{aw}}BG(x) - h(x_{aw})'W\right] & 0 \\ \star & \left(W - \frac{\varepsilon}{2}I\right) & -\frac{1}{2}W \\ \star & \star & -\gamma^2 I \end{bmatrix} < 0 \quad (38)$$

*Proof:* The first part of the proof is similar to the IMC case: we arrive at expression (21), showing that the auxiliary signal is canceled in the error dynamics. Next note that:

$$\sup_{w \neq 0} \frac{\|z\|_2}{\|w\|_2} = \sup_{w \neq 0} \frac{\|C_z x\|_2}{\|w\|_2} \quad (39)$$

$$\leq \sup_{w \neq 0} \frac{\|C_z x_{aw}\|_2}{\|w\|_2} + \sup_{w \neq 0} \frac{\|C_z e\|_2}{\|w\|_2} \quad (40)$$

However, as  $e(t)$  is independent [this fact can be easily derived via the computation of the error dynamics, similar to Eq. (19)] of  $w$ ,  $\|Ce\|_2$  is constant and hence:

$$\sup_{w \neq 0} \frac{\|C_z e\|_2}{\|w\|_2} = 0 \quad (41)$$

Thus, we have

$$\sup_{w \neq 0} \frac{\|z\|_2}{\|w\|_2} \leq \sup_{w \neq 0} \frac{\|C_z x_{aw}\|_2}{\|w\|_2} \quad (42)$$

and hence, it is sufficient to study the dynamics of the AW compensator for performance analysis. Picking  $V(x_{aw}) > 0$ , see Eqs. (24–26), for  $x_{aw} \in \mathcal{C}$  as a Lyapunov function for the system, we investigate

$$\dot{V}(x_{aw}) + \|C_z x_{aw}\|^2 - \gamma^2 \|w\|^2 \quad (43)$$

to obtain the asymptotic stability and the required  $\mathcal{L}_2$  gain property.

Appending the sector condition  $\tilde{u}'W(u - \tilde{u}) \geq 0$ , where  $\tilde{u} = Dz(u)$ , to Eq. (43), and substituting for  $\dot{x}_{aw}$ , an upper bound on Eq. (43) is as follows:

$$\begin{aligned} \frac{\partial V}{\partial x_{aw}}[Ax_{aw} + Bf(x_{aw}) + BG(x)h(x_{aw})] + x'_{aw}C'_z C_z x_{aw} \\ + \frac{\partial V}{\partial x_{aw}}BG(x)\tilde{u} - \tilde{u}'Wh(x_{aw}) - \tilde{u}'W\tilde{u} - \tilde{u}'Ww - \gamma^2 w'w \\ + \tilde{u}'WG(x)^{-1}[f(x) - f(x_{aw}) - D_c C(x - x_{aw}) \\ - C_c x_c - D_{cr} r - BD_c D_{pd} d] \end{aligned} \quad (44)$$

However, using the inequality  $2v'V'Yy \leq \varepsilon v'V'Vv + \varepsilon^{-1}y'Y'Yy$  for all  $\varepsilon > 0$ , this implies another upper bound for Eq. (43) and  $x_{aw} \in \mathcal{C}$ :

$$\begin{aligned} \frac{\partial V}{\partial x_{aw}}[Ax_{aw} + Bf(x_{aw}) + BG(x)h(x_{aw})] + x'_{aw}C'_z C_z x_{aw} - \gamma^2 w'w \\ + \frac{\partial V}{\partial x_{aw}}BG(x)\tilde{u} - \tilde{u}'Wh(x_{aw}) - \tilde{u}'\left(W - \frac{\varepsilon}{2}I\right)\tilde{u} - \tilde{u}'Ww \\ + \frac{1}{2\varepsilon} \|WG(x)^{-1}\|^2 \|f(x) - f(x_{aw})\|^2 - D_c C(x - x_{aw}) \\ - C_c x_c - D_{cr} r - BD_c D_{pd} d \|^2 \end{aligned} \quad (45)$$

Thus, to guarantee local stability, i.e.,  $x_{aw} \in \mathcal{C}$ , a small signal argument needs to be made, as done for Theorem 1.

By integrating the whole of Eq. (45) over the interval  $(0, \infty)$ , the upper bound of the  $\mathcal{L}_2$  norm of the last term of Eq. (45) is finite, assuming a finite  $\mathcal{L}_2$ -norm for  $r$  and  $d$  in an  $\mathcal{L}_2$ -analysis and using Eq. (21). In the case the relationship of inequality (38) is satisfied, it follows that the map  $\mathcal{T}_p: w \mapsto z$  has an  $\mathcal{L}_2$  gain less than  $\gamma$ , as the sum of the first three terms of Eq. (45) is less than or equal to zero, and equivalent to that of inequality (38). To guarantee that this is valid in a local sense, a small signal argument again for  $\|\hat{W}\|$  applies so that the last term of Eq. (45) remains in bound small. The same applies to the signal bounds of  $w$  for the first three terms of Eq. (45). For reasons of brevity, further discussions are here avoided as they are standard.

The problem of minimizing  $\gamma$  subject to inequality (38) is difficult, and is unlikely to be convex. It is possible to search directly for  $V(x_{aw})$  and  $h(x_{aw})$ , but this task can be made easier by imposing a

structure on  $h(x_{aw})$ . Taking inspiration from optimal control, an appealing choice is  $h(x_{aw}) = -G(x)'B'\partial V(x_{aw})/\partial x_{aw}$ . Such a choice simplifies the solution of our inequality (38) by reducing the complexity of the search. Moreover, the choice of  $h(x_{aw})$ , which is parametrized through the open loop Lyapunov function, ensures its contribution to the inequality (38) to be nonpositive for all  $x_{aw} \neq 0$ . Thus, it introduces a stabilizing nonlinear damping term, as discussed in ([49] pp. 539, 588).

#### IV. Experimental Results

This section describes the experimental testing of the NDI AW schemes. The nominal unconstrained control law used is,

$$u = \frac{1}{M_\eta} [-(M_\theta\theta + M_q q) + u_{lin}] \quad (46)$$

where  $u_{lin}$  is the linear outer loop PID control law ensuring the robust set point tracking

$$u_{lin} = 32.5\theta_e + 7 \int \theta_e dt + 10 \frac{d\theta_e}{dt} \quad (47)$$

where  $\theta_e = (\theta_r - \theta)$  represents the signal generated from the reference  $\theta_r$ , and the pitch measurement  $\theta$ . The gains are selected to have two complex poles representing the short period dynamics. The control gains are tuned to ensure robust performance in the presence of significant amount of disturbances in the openjet wind tunnel as mentioned earlier. The NDI inner and linear outer loop combination provide desirable robust tracking performance. These are implemented using a dSPACE real-time interface. A fourth-order, stable infinite impulse response filter is introduced to filter the measured pitch angle signal obtained from the wind tunnel using the dSPACE data acquisition. The rotational velocity signal is not measured directly but is computed numerically using differentiation and then filtered.

##### A. Nominal Control Without and with Actuator Limits

The nominal response of the controller to the tracking signal is given in Fig. 4. The reference signal is given as 'REF' (blue dashed lines) and nominal response as 'Nominal' (black bold line), respectively. The initial reference operating region is fixed at  $\eta = 4$  deg tailplane deflection. In the unconstrained case, the present nonlinear controller tracks the reference command well with no overshoot. However, there is a 3.5 s delay in tracking the reference signal. For studying the AW architectures, the saturation limits  $[-3.75 \text{ deg}, 4.75 \text{ deg}]$  are introduced. In the presence of saturation, the performance of the nominal nonlinear controller deteriorates to that shown by the bold dash dotted line in Fig. 4 (given as case 'SAT' in red).

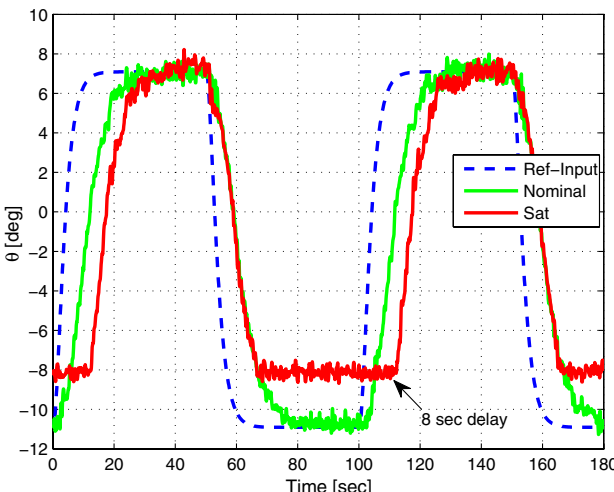


Fig. 4 Reference input, nominal and saturated  $\theta(t)$  response; delay between nominal and saturated response 8 s.

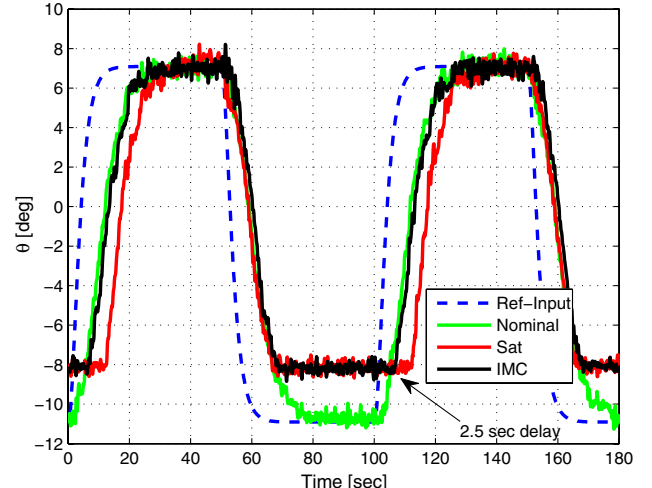


Fig. 5 Performance recovery using IMC compensation scheme; delay between nominal and saturated response 2.5 s.

in red). Observe the significant amount of time lag and the slight overshoot in tracking the reference signal in the presence of the amplitude saturation. The saturated signal has a time lag of 8 s (as marked in Fig. 4) relative to the nominal response, i.e., a 11.5 s delay relative to the tracking signal.

##### B. IMC AW Compensation and Results

For AW design, the mathematical model for the Hawk aircraft, Eq. (1), suits the compensator synthesis approach by choosing:

$$A = 0, \quad B = \begin{bmatrix} 1 \\ 0 \end{bmatrix},$$

$$f(\theta, \dot{\theta}) = M_q(\theta, \dot{\theta}, \tilde{\eta})|_{\tilde{\eta}=4} q + M_\theta(\theta, \dot{\theta}, \tilde{\eta})|_{\tilde{\eta}=4} \theta,$$

$$G(\theta, \dot{\theta}) = M_\eta(\theta, \dot{\theta}, \tilde{\eta})|_{\tilde{\eta}=4} \quad (48)$$

Hence, the IMC AW compensator, i.e.,  $h(x_{aw}) = 0$  in Eqs. (10) and (11), can be introduced for compensation of the effects due to violation of constraints. The black bold line in Fig. 5 shows the pitch angle response of the closed-loop system with the IMC AW compensation scheme. Although the stability is ensured and performance has been improved relative to no AW, the IMC AW scheme still introduces a 2.5 s delay with respect to the nominal control response (compared to the 8 s delay in the saturated case) while tracking the reference signal (i.e., this shortened the overall delay with respect to the tracking signal to 6 s). The nominal response is given in a dotted green line in Fig. 5.

##### C. Optimal NDI AW Compensator Design

The optimal NDI AW compensation scheme is developed as given in Eqs. (10) and (11). The significant difference to the IMC scheme in Eqs. (15) and (16) is the introduction of the additional signal  $h(x_{aw})$ . The closed-loop system with the optimal AW architecture is shown in Fig. 3. The additional signal is  $h(x_{aw}) = -G(x)'B'\partial V(x_{aw})/\partial x_{aw}$ ; it depends on  $V$ , which acts also as an open-loop Lyapunov function. However, to ensure performance of the AW scheme, i.e.,  $\mathcal{L}_2$  performance, the compensation synthesis is necessarily formulated as an optimization procedure, minimizing the  $\mathcal{L}_2$  gain subject to the matrix inequality as given in inequality (38) of Theorem 2. The matrix inequality constraint considered here is no longer linear or convex and hence cannot be solved using LMI methods as was done in previous linear AW compensator designs in [24,37]. The algorithm, proposed in this paper, is iterative and makes use of a two-stage optimization process to obtain the extended quadratic form Lyapunov matrix satisfying the  $\mathcal{L}_2$  optimization constraints defined in inequality (38). Hence, the optimization problem is solved using an evolutionary global optimization procedure called genetic algorithms (GA) [53]. A ' $\delta$ ' term is introduced for optimization purposes and the matrix inequality given in inequality (38) is rewritten in the form

$[ML] \leq -\delta[MR]$ , where  $[ML]$  represents inequality (38) itself and  $[MR]$  is as follows:

$$\begin{bmatrix} -\frac{\partial V}{\partial x_{aw}} [Ax_{aw} + Bf(x_{aw})] & 0 & 0 \\ 0 & I & 0 \\ 0 & 0 & I \end{bmatrix} \quad (49)$$

From inequality (49), the  $\delta$  term is used to ensure that the right hand side of the inequality  $[ML] \leq -\delta[MR]$  is negative definite. This enforces that the left hand  $[ML]$  is also negative definite, i.e., excludes singular and infeasible cases. It facilitates in particular the two-step algorithm as detailed in Algorithm 1 similar to a (nonconvex) max-min type optimization problem.

#### Algorithm 1 Optimization procedure algorithm

- 
1. Fix  $\gamma$  to a large value to start with, say 100
  - STEP 1**
  2. Assign nonzero initial values for the controller and compensator states ( $x = 0, x_{aw} = 0$ ) for a given operating region (i.e., the compact set  $C$  in Theorems 1 and 2)
  3. Initialize  $N$  random Lyapunov candidate matrix ( $P_i$ ) entries
  4. While the termination criteria are satisfied
    - a)  $\forall P_i, i = 1 \dots N$ , search for the largest  $\delta$  satisfying the matrix inequalities; Assign the largest  $\delta$  as the fitness associated with  $P_i$
    - b) Apply GA operators and continue search for the  $P_i$  with largest  $\delta$
  5. end of While
  - STEP 2**
  6. Fix the  $P^*$ , obtained from *STEP 1*
  7. Initialize  $N$  random controllers and compensator state values ( $[x^i, x_{aw}^i]$ ) within the chosen operating region
  8. While the termination criteria are satisfied
    - a)  $\forall [x^i, x_{aw}^i], i = 1 \dots N$ , search for the smallest  $\delta$  satisfying the matrix inequalities; Assign the smallest  $\delta$  as the fitness associated with  $[x^i, x_{aw}^i]$
    - b) Apply GA operators and continue search for the  $[x^i, x_{aw}^i]$  with the smallest  $\delta$
  9. end of While
  10. Choose the worst  $[x^i, x_{aw}^i]$ , reduce  $\gamma$  and repeat *STEP 1* and check
  11. Terminate once *STEP 2* has no solution for  $\delta > 0$  and use prior solution for  $h(\cdot)$
- 

*Remark 1:* In the linear case, the Lyapunov function  $V(x_{aw})$  is typically chosen to be a quadratic function, and the  $L_2$  gain minimization is treated using LMI techniques. However, in the nonlinear case, the convexity of the minimization is not guaranteed and typically cannot be solved with LMIs. Here, due to the nature of the chosen optimization algorithm, it is possible to choose a more sophisticated extended quadratic, i.e., higher-order Lyapunov function such as  $V(x_{aw}, k) \geq 0$ ,

$$V(x_{aw}, k) = \begin{bmatrix} x_{aw} \\ \nu(x_{aw}, 2) \\ \vdots \\ \nu(x_{aw}, k) \end{bmatrix}^T \underbrace{\begin{bmatrix} P_{11} & P_{12} & \dots & P_{1k} \\ P_{12}^T & P_{22} & \dots & P_{2k} \\ \vdots & \vdots & \ddots & \vdots \\ P_{1k}^T & P_{2k}^T & \dots & P_{kk} \end{bmatrix}}_P \begin{bmatrix} x_{aw} \\ \nu(x_{aw}, 2) \\ \vdots \\ \nu(x_{aw}, k) \end{bmatrix} > 0, \quad (50)$$

$(x_{aw} \neq 0)$

where the vector function  $\nu(x_{aw}, i) \in \mathbb{R}^n$  denotes:

$$\nu(x_{aw}, i) := [x_{aw,1}^i \quad x_{aw,2}^i \quad \dots \quad x_{aw,n}^i]^T \quad (51)$$

This choice may provide a smaller value of  $\gamma > 0$ . In the case of this paper, a simple quadratic Lyapunov function,  $V(x_{aw}) = x_{aw}^T P x_{aw}$ , is shown to be sufficient to obtain an AW compensator which significantly improves the performance recovery over the IMC case. A quadratic Lyapunov function is also sufficient to show typical characteristics of the tuning tools available to this AW design approach.

The number of optimization variables essentially depends on two factors: 1) the order of the Lyapunov function, presently quadratic (the order can have an extended form), and 2) the order of the state variables of the nonlinear system. The optimization has the following rationale: initially  $\gamma$  is fixed at a large value, and the optimization searches for the entries of the Lyapunov candidate matrix, subject to the matrix inequality constraints guaranteeing stability and performance.

In *STEP 1*, the intention is to fix  $x$  and  $x_{aw}$  and to obtain the Lyapunov matrix via GA that could provide a maximum of  $\delta$  (see short explanation below). It is expected that a large value of  $\delta$  guarantees that the left hand side  $[ML]$  remains negative definite for fixed Lyapunov candidate, when (in *STEP 2*) the inequality (49) is tested for a large number of  $x$  and  $x_{aw}$  values in the region of interest (i.e., within the original controller operation area). Thus, the GA in *STEP 1* introduces chromosomes, the optimization vector, which is the minimum number of Lyapunov matrix entries; For the present quadratic Lyapunov function, we have three entries.  $N$  random symmetric positive definite ‘Lyapunov’ matrices  $P_i, i = 1, \dots, N$ , as in Eq. (50), are generated. A sufficiently large number of initial candidates are necessary to ensure an initial coverage of the search space and thus the convergence of the evolving population [53]. The search begins with these randomly generated Lyapunov matrices. For each of the candidate Lyapunov matrices, the largest possible  $\delta$  satisfying the matrix inequality constraints  $[ML] \leq -\delta[MR] < 0$  is sought. The largest value of  $\delta$  associated with each candidate Lyapunov matrix is assigned as the fitness for each of the  $P$  matrices. GA operators are applied and the search continues for the  $P$  matrix with the largest  $\delta$ . A simple GA with single point crossover and binary mutation operators is used. A maximum number of generations, fixed at 100, is applied as the termination criterion for the search in both steps. Also, the number of candidates in the initial population is fixed at  $N = 50$ . The candidates from the present generation are qualified to produce the successive generations depending on a normalized geometric ranking selection scheme with a selection probability of 0.08. The single point crossover with a probability of crossover fixed at 0.75, and binary mutation with low probability of mutation, fixed at 0.05, are used in both optimization steps. Once a Lyapunov candidate matrix  $P$  is obtained from the GA search in the first step (*STEP 1*), that matrix  $P$  is kept fixed in the second step of the two step procedure (*STEP 2*).

In *STEP 2*, the worst case values for  $x$  and  $x_{aw}$  are found to find the worst case  $\delta$  for fixed  $P$ . In case inequality (49) is not satisfied for positive value  $\delta$ , the solution  $h(\cdot)$  is not feasible. In any other case, a reduced  $\gamma$  will be used to go back to *STEP 1* to obtain a better  $h(\cdot)$ . Hence, the GA optimization variable vector consists of the controller and compensator state values. The initial and maximum number of chromosomes is as in *STEP 1*. Note that reasonable bounds are chosen for the values of the states, based on the initial invariant set under consideration; usually a sufficiently large superset is chosen to satisfy inequality (49). The smallest  $\delta$  satisfying the same matrix inequality constraints is assigned as the fitness to each candidate controller and compensator state vector. The GA optimization over iterations finds the maximum controller and compensator state values with the smallest  $\delta$ . Then the solution is checked by repeating the procedure and successively reducing the value  $\gamma$ . The details of the optimization algorithm for the compensator design are summarized in the Algorithm 1. The value of  $\epsilon$  is kept very low, fixed at 0.01.

#### D. Optimal NDI AW Compensation Results

Following the optimization procedure described in Sec. IV.C, an AW compensator was designed which minimized the  $L_2$  performance bound  $\gamma$  for

$$z = C_z x = \begin{bmatrix} 1 & 0 \\ 0 & 1 \end{bmatrix} \begin{bmatrix} q \\ \theta \end{bmatrix} \quad (52)$$

The weighting was chosen as identity matrix of order 2, implying equal importance on performance outputs. In this case, a quadratic,

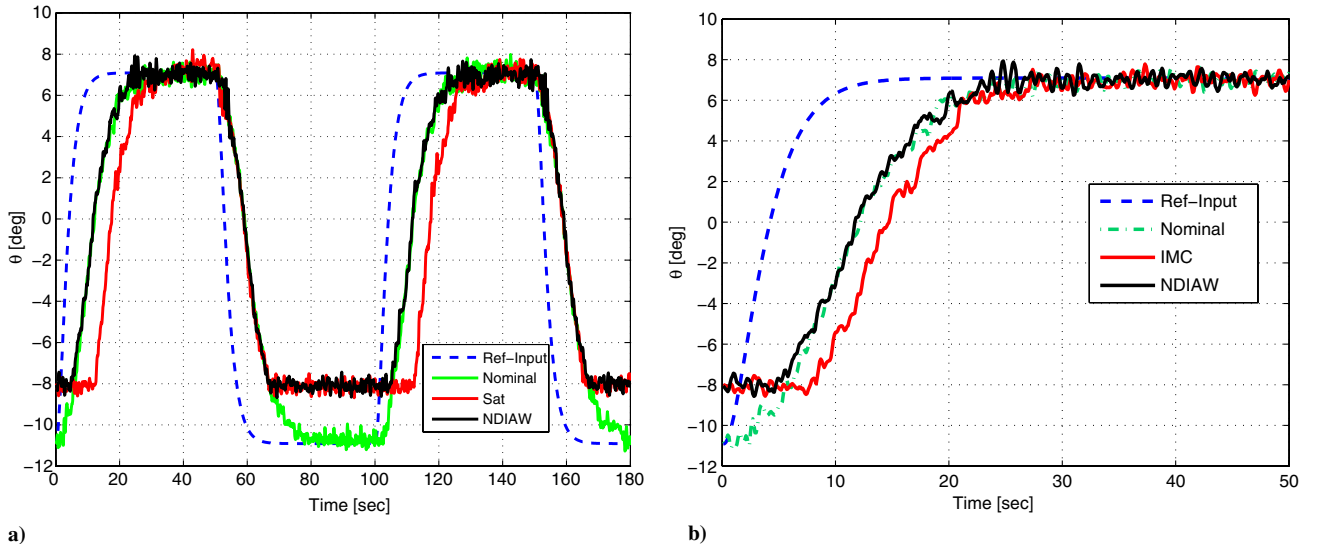


Fig. 6 Performance recovery using IMC and optimal NDI AW compensation schemes.

positive definite Lyapunov function was sufficient and the value returned by the optimization procedure was:

$$V(x_{aw}) = [x_{aw}]' \underbrace{\begin{bmatrix} 0.2576 & 0.0894 \\ 0.0894 & 0.8660 \end{bmatrix}}_P [x_{aw}] \quad (53)$$

The associated value of  $\gamma$  was 0.32 and the search for this Lyapunov function was confined to the box  $|x_i|, |x_{aw,i}|$  for  $i = 1, 2$  using the intervals

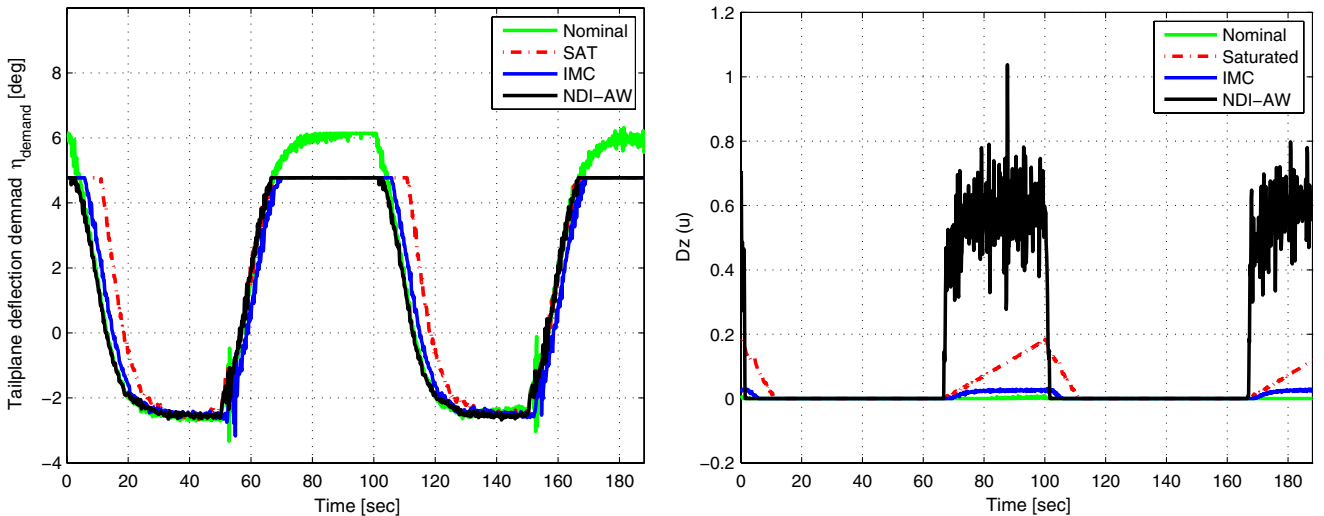
$$\theta \in [-20, 40], \quad q \in [-150, 150] \quad (54)$$

as bounds (i.e., the expected operating region of the Algorithm 1) for  $\theta$  and  $q$ . Note that in the optimization, the states of controller and compensator are bounded. Hence, stability and in particular the  $L_2$  gain is computed locally. Considering that the condition number of  $P$  is 3.6 in Eq. (53) and the investigated set of intervals (54), a worst case set where the  $L_2$  gain of 0.32 holds is a circle in  $(\theta, q)$  with a radius of at least 10. Considering the practically evaluated performance for  $(\theta, q)$ , this set is practically sensible.

The black bold line in Fig. 6a shows the pitch angle response of the closed-loop system with optimal full-order NDI AW compensation scheme. The performance of the nominal closed-loop system has

been completely recovered, while the saturation nonlinearity is active. There is no delay in tracking the signal in presence of saturation compared to the nominal response. In the transient region as well, the optimal NDI AW scheme shows no oscillatory response, completely restoring the nominal control performance compared to the IMC AW scheme. This clearly demonstrates that the NDI AW using the  $L_2$  performance optimization is much more advantageous over the baseline IMC scheme. Figure 6b shows the comparison of the performance recovery with the proposed two different AW schemes during the transient region of the pitch angle tracking.

The tailplane deflection demand  $\eta_{\text{demand}}$  corresponding to nominal, saturated, IMC compensated and optimal NDI AW compensated cases are shown in Fig. 7a. Note that the tailplane deflection demands  $\eta_{\text{demand}}$  are amplitude limited to 4.75 deg by imposing the artificial saturation to demonstrate and compare the effectiveness of the different methodologies. The phase lag associated with the IMC compensation scheme can also be observed in Fig. 7. The deadzone signal  $Dz(u)$  in case of the nominal (green bold), saturated (red bold), IMC compensated (blue bold), and the optimal NDI AW compensated (black bold) is given in Fig. 7b. In case of saturation without AW, the figure implies that the control signal  $u(t)$  prior to saturation is winding up. It can be seen that in the case of optimal NDI AW the control signal makes use of the operation on the limits to recover the performance, i.e.,  $Dz(u)$  returns quickly to zero. It is important to mention that it is quite normal to have an aggressive control signal



a) Tailplane deflection demand  $\eta_{\text{demand}}(t)$  (deg)

Fig. 7 Nominal and saturated control, IMC and NDI AW response for design of Eq. (52).

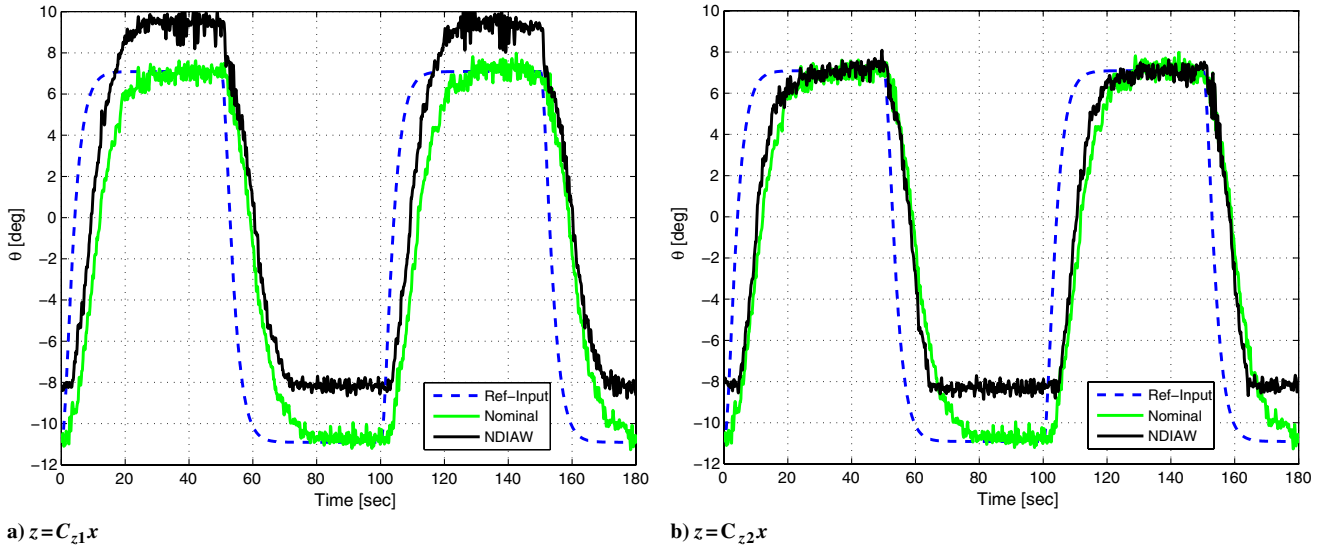


**Fig. 8 Performance tuning using the optimal NDI AW compensation schemes.**

$u(t)$ , i.e., also  $Dz(u)$ . In particular, the control signal  $u(t)$  is clipped by the artificial AW saturation-element as it does not affect the actuator signal, i.e., in our case the tailplane deflection demand  $\eta_{\text{demand}}$ . It is easily seen in Fig. 7b that the NDI AW signal recovers faster from saturation than the controller without AW compensation or with IMC AW compensation, at time instance  $t = 102$  s.

#### E. Weighting Matrix: A Tool for Performance Tuning

Compared to the identical weighting given in Eq. (52), consider different weightings for the performance outputs as

$$z = C_{z1}x = \begin{bmatrix} 1 & 0 \\ 0 & 0.1 \end{bmatrix} \begin{bmatrix} q \\ \theta \end{bmatrix} \quad (55)$$

implying higher importance on the pitch rate performance output, even though the desired tracking performance requirements are for the pitch angle. In this case, another quadratic, positive definite Lyapunov function was obtained by the optimization procedure:

$$V(x_{\text{aw}}) = [x_{\text{aw}}]' \underbrace{\begin{bmatrix} 0.2514 & -0.018 \\ -0.018 & 0.0392 \end{bmatrix}}_P [x_{\text{aw}}] \quad (56)$$

The performance value obtained was  $\gamma = 0.87$  and the search for this Lyapunov function was confined to the original box  $|x_i|, |x_{\text{aw},i}|$  for  $i = 1, 2$  using the intervals

$$\theta \in [-20, 40], \quad q \in [-150, 150]$$

as bounds for  $\theta$  and  $q$ . Considering the principal directions of  $P$ , the  $L_2$  gain  $(\theta, q)$  again is valid in a local set in  $(\theta, q)$  forming a circle with a radius of at least 10.

The black bold line in Fig. 8a shows the pitch angle response of the closed-loop system with optimal full-order NDI AW compensation scheme. Because the higher weighting on term  $q$ , an overshoot/significant steady state error can be seen in the performance of the AW compensated case. However, there is no significant delay in tracking the reference signal in the presence of saturation compared to the nominal response.

Consider an alternate case, where the weighting on the pitch rate is reduced but normal weighting is maintained for the pitch angle:

$$z = C_{z2}x = \begin{bmatrix} 0.1 & 0 \\ 0 & 1 \end{bmatrix} \begin{bmatrix} q \\ \theta \end{bmatrix} \quad (57)$$

implying a 10 times higher importance for the pitch angle performance output than the pitch rate signal. In this case, another

quadratic, positive definite Lyapunov function was obtained by the optimization procedure:

$$V(x_{\text{aw}}) = [x_{\text{aw}}]' \underbrace{\begin{bmatrix} 1.179 & 1.156 \\ 1.156 & 2.3726 \end{bmatrix}}_P [x_{\text{aw}}] \quad (58)$$

The associated performance value was  $\gamma = 0.5$ , which equally is valid in a circle in  $(\theta, q)$  with a radius of 10. Because the  $\theta(t)$  term has a higher weight compared to that of  $q$ , it can be seen from Fig. 8b that the compensator is able to recover the performance in the presence of actuator saturation. A designer can thus fine tune the compensator performance, as in a classical sense, considering in this case the parameters in the weighting matrix  $C_z$ .

#### V. Conclusions

In this paper, a recently developed NDI AW scheme has been applied to a realistic aerospace application, a scaled approximate wind-tunnel model of the BAe Hawk aircraft. The results of a real-time wind-tunnel implementation of the NDI AW scheme demonstrate the effectiveness of the method. It is shown that the NDI AW scheme performs better than the useful, but limited, IMC AW scheme. To the authors' knowledge, this is the first realistic aerospace application and demonstration of the effectiveness of a systematic nonlinear AW compensation design scheme along with the industrially favored NDI scheme. Moreover, the level of disturbances and nonlinearities present in the model demonstrates the potential of the methodology. An original framework for tuning the performance of the compensation scheme is clearly demonstrated by wind-tunnel experiments. This resembles strongly the understanding of linear control principles, i.e., PID or in particular mixed sensitivity linear  $H_\infty$ -control; e.g., large weighting of position related performance outputs improve nominal control recovery in steady state. Thus, the suggested NDI AW scheme allows tuned recovery of the nominal control response.

#### References

- [1] Bugajski, J., and Enns, F., "Nonlinear Control Law with Application to High Angle of Attack Flight," *Journal of Guidance, Control, and Dynamics*, Vol. 15, No. 3, 1992, pp. 761–767.  
doi:10.2514/3.20902
- [2] Enns, F., Bugajski, D., Hendrick, R., and Stein, G., "Dynamic Inversion: An Evolving Methodology for Flight Control Design," *International Journal of Control*, Vol. 59, No. 1, 1992, pp. 71–91.  
doi:10.1080/00207179408923070
- [3] Reiner, J., Balas, G., and Garrard, W., "Flight Control Design Using Robust Dynamic Inversion and Time Scale Separation," *Automatica*,

- Vol. 32, No. 11, 1996, pp. 1493–1504.  
doi:10.1016/S0005-1098(96)00101-X
- [4] Ito, D., Ward, D., and Valasek, J., “Robust Dynamic Inversion Controller Design for the X-38,” AIAA Paper 2001-4380, 2001.
- [5] Georgie, J., and Valasek, J., “Evaluation of Longitudinal Desired Dynamics for Dynamic Inversion Controlled Generic Reentry Vehicles,” *Journal of Guidance, Control, and Dynamics*, Vol. 26, No. 5, 2003, pp. 811–819.  
doi:10.2514/2.5116
- [6] Snell, S., Enns, D., and Garrard, W., “Nonlinear Inversion Flight Control for a Supermaneuverable Aircraft,” *Journal of Guidance, Control, and Dynamics*, Vol. 15, No. 4, 1992, pp. 1301–1305.  
doi:10.2514/3.20932
- [7] Snell, A., and Stout, W., “Flight Control Law Using Dynamic Inversion Combined with Quantitative Feedback Theory,” *Journal of Dynamic Systems, Measurement and Control*, Vol. 120, No. 7, 1998, pp. 208–214.  
doi:10.1115/1.2802411
- [8] Escande, B., “HIRM Design Challenge Presentation Document: The Nonlinear Dynamics Inversion and Linear Quadratic Approach,” Group for Aeronautical Research and Technology in Europe, TR-088-30, 1997.
- [9] Bennani, S., and Looye, G., “Flight Control Law Design for a Civil Aircraft Using Robust Dynamic Inversion,” *Proceedings of IEEE/SMC-CESA 98 Congress*, Tunisia, 1998.
- [10] Papageorgiou, G., and Hyde, R., “Analysing the Stability of NDI-Based Flight Controllers with LPV Methods,” AIAA Paper 2001-4380, 2001.
- [11] Papageorgiou, G., and Glover, K., “Robustness Analysis of Nonlinear Flight Controllers,” *Journal of Guidance, Control, and Dynamics*, Vol. 28, No. 4, 2005, pp. 639–648.  
doi:10.2514/1.9389
- [12] Smith, P., and Berry, A., “Flight Test Experience of Nonlinear Dynamic Inversion Control Law on the VAAC Harrier,” AIAA Paper 2000-3914, 2000.
- [13] Valasek, J., Akella, M., Siddarth, A., and Rollins, E., “Adaptive Dynamic Inversion Control of Linear Plants with Control Position Constraints,” *IEEE Transactions on Control Systems Technology*, Vol. 20, No. 4, 2012, pp. 918–933.  
doi:10.1109/TCST.2011.2159976
- [14] Hanus, R., Kinnaert, M., and Henrotte, J., “Conditioning Technique, a General Anti-windup and Bumpless Transfer Method,” *Automatica*, Vol. 23, No. 4, 1987, pp. 729–739.  
doi:10.1016/0005-1098(87)90029-X
- [15] Kothare, M. V., Campo, P. J., Morari, M., and Nett, C. N., “A Unified Framework for the Study of Anti-Windup Designs,” *Automatica*, Vol. 30, No. 12, 1994, pp. 1869–1883.  
doi:10.1016/0005-1098(94)90048-5
- [16] Hippe, P., and Wurmthaler, C., “Systematic Closed-Loop Design in the Presence of Input Saturation,” *Automatica*, Vol. 35, No. 4, 1999, pp. 689–695.  
doi:10.1016/S0005-1098(98)00199-X
- [17] Glattfelder, A., and Schaufelberger, W., *Control of Systems with Input and Output Constraints*, Springer-Verlag, Berlin, 2003.
- [18] Teel, A., and Kapoor, N., “The  $\mathcal{L}_2$  Anti-Windup Problem: Its Definition and Solution,” *Proceedings of the European Control Conference*, Brussels, Belgium, 1997, pp. 1–4.
- [19] Grimm, G., Postlethwaite, I., Teel, A., Turner, M., and Zaccarian, L., “Linear Matrix Inequalities for Full and Reduced Order Anti-Windup Synthesis,” *Proceedings of American Control Conference*, Arlington, VA, 2001, pp. 4134–4139.
- [20] Weston, P., and Postlethwaite, I., “Analysis and Design of Linear Conditioning Schemes for Systems Containing Saturating Actuators,” *IFAC Nonlinear Control System Design Symposium*, Enschede, The Netherlands, 1998, pp. 702–707.
- [21] Gomes Da Silva, J. M. Jr., Tarbouriech, S., and Reginatto, R., “Analysis of Regions of Stability for Linear Systems with Saturating Inputs Through an Anti-Windup Scheme,” *Proceedings of IEEE CCA*, Glasgow, Scotland, UK, 2002, pp. 1106–1111.
- [22] Crawshaw, S., and Vinnicombe, G., “Anti-Windup Synthesis for Guaranteed  $\mathcal{L}_2$  Performance,” *Proceedings of IEEE CDC*, Sydney, Australia, 2000, pp. 1063–1068.
- [23] Grimm, G., Postlethwaite, I., Teel, A., Turner, M., and Zaccarian, L., “Case Studies Using Linear Matrix Inequalities for Optimal Anti-Windup Compensator Synthesis,” *European Journal of Control*, Vol. 9, No. 5, 2003, pp. 463–473.  
doi:10.3166/ejc.9.463-473
- [24] Turner, M., and Postlethwaite, I., “A New Perspective on Static and Low Order Anti-Windup Synthesis,” *International Journal of Control*, Vol. 77, No. 1, 2004, pp. 27–44.  
doi:10.1080/00207170310001640116
- [25] Turner, M. C., Herrmann, G., and Postlethwaite, I., “Incorporating Robustness Requirements into Anti-Windup Design,” *IEEE Transactions on Automatic Control*, Vol. 52, No. 10, 2007, pp. 1842–1855.  
doi:10.1109/TAC.2007.906185
- [26] Gomes da Silva, J. Jr., Tarbouriech, S., and Garcia, G., “Local Stabilisation of Linear Systems Under Amplitude and Rate Saturating Actuators,” *IEEE Transactions on Automatic Control*, Vol. 48, No. 5, 2003, pp. 842–847.  
doi:10.1109/TAC.2003.811265
- [27] Barbu, C., Galeani, S., Teel, A. R., and Zaccarian, L., “Non-Linear Anti-Windup for Manual Flight Control,” *International Journal of Control*, Vol. 78, No. 14, 2005, pp. 1111–1129.  
doi:10.1080/00207170500267929
- [28] Herrmann, G., Turner, M. C., Postlethwaite, I., and Guo, G., “Practical Implementation of a Novel Anti-Windup Scheme in a HDD-Dual-Stage Servo-System,” *IEEE/ASME Transactions on Mechatronics*, Vol. 9, No. 3, 2004, pp. 580–592.  
doi:10.1109/TMECH.2004.835333
- [29] Zaccarian, L., and Teel, A., *Modern Anti-Windup Synthesis: Control Augmentation for Actuator Saturation*, Princeton Series in Applied Mathematics, Princeton Univ. Press, Princeton, NJ, 2011, pp. 245–268, Chap. 10.
- [30] Tarbouriech, S., Garcia, G., Gomes da Silva, J. Jr., and Queinnec, I., *Stability and Stabilization of Linear Systems with Saturating Actuators*, Springer-Verlag, London, 2011.
- [31] Galeani, S., Tarbouriech, S., Turner, M., and Zaccarian, L., “A Tutorial on Modern Anti-Windup Design,” *European Journal of Control*, Vol. 15, Nos. 3–4, 2009, pp. 418–440.  
doi:10.3166/ejc.15.418-440
- [32] Tarbouriech, S., and Turner, M., “Anti-Windup Design: An Overview of Some Recent Advances and Open Problems,” *IET Control Theory Application*, Vol. 3, No. 1, 2009, pp. 1–19.  
doi:10.1049/iet-cta:20070435
- [33] Kahveci, N., Ioannou, P., and Mirmirani, M., “Adaptive LQ Control with Anti-Windup Augmentation to Optimize UAV Performance in Autonomous Soaring Applications,” *IEEE Transactions on Control Systems Technology*, Vol. 16, No. 4, 2008, pp. 691–707.  
doi:10.1109/TCST.2007.908207
- [34] Pavlov, A., Pogromsky, A., van deWouw, N., and Nijmeijer, H., “Convergent Dynamics, a Tribute to Boris Pavlovich Demidovich,” *Systems and Control Letters*, Vol. 52, Nos. 3–4, 2004, pp. 257–261.  
doi:10.1016/j.sysconle.2004.02.003
- [35] Herrmann, G., Menon, P., Turner, M., Bates, D., and Postlethwaite, I., “Anti-Windup Synthesis for Nonlinear Dynamic Inversion Control Schemes,” *International Journal of Robust and Nonlinear Control*, Vol. 20, No. 13, 2010, pp. 1465–1482.  
doi:10.1002/rnc.1523
- [36] Weston, P., and Postlethwaite, I., “Linear Conditioning for Systems Containing Saturating Actuators,” *Automatica*, Vol. 36, No. 9, 2000, pp. 1347–1354.  
doi:10.1016/S0005-1098(00)00044-3
- [37] Turner, M., Herrmann, G., and Postlethwaite, I., “Accounting for Uncertainty in Anti-Windup Synthesis,” *Proceedings of ACC*, Boston, MA, 2004, pp. 5292–5297.
- [38] Herrmann, G., Turner, M. C., and Postlethwaite, I., “Discrete-Time and Sampled Data Anti-Windup Synthesis: Stability and Performance,” *International Journal of Systems Science*, Vol. 37, No. 2, 2006, pp. 91–113.  
doi:10.1080/0020772050044074
- [39] Queinnec, I., Tarbouriech, S., and Garcia, G., “Anti-Windup Design for Aircraft Flight Control,” *IEEE Conference on Control Applications*, Munich, Germany, 2006, pp. 2541–2546.
- [40] Sofrony, J., Turner, M. C., Postlethwaite, I., Brieger, O., and Leissling, D., “Anti-Windup Synthesis for PIO Avoidance in an Experimental Aircraft,” *Proceedings of 45th IEEE Conference on Decision and Control*, San Diego, CA, 2006, pp. 5412–5417.
- [41] Brieger, O., Kerr, M., Leissling, D., Postlethwaite, I., Sofrony, J., and Turner, M., “Anti-Windup Compensation of Rate Saturation in an Experimental Aircraft,” *Proceedings of American Control Conference*, New York, NY, 2007, pp. 924–929.
- [42] Davison, P., Lowenberg, M., and di Bernardo, M., “Experimental Analysis and Modelling of Limit Cycles in a Dynamic Wind Tunnel,” *Journal of Aircraft*, Vol. 40, No. 4, 2003, pp. 776–785.  
doi:10.2514/2.3158
- [43] Davison, P., di Bernardo, M., and Lowenberg, M., “Modelling and Control of a Single Degree of Freedom Dynamic Wind Tunnel Rig,”

- Proceedings of the European Control Conference*, Cambridge, U.K., 2003, pp. 597–602.
- [44] Richardson, T., Lowenberg, M., Jones, C., and Dubs, A., “Dynamic Gain Scheduled Control of a Hawk Scale Model,” *The Aeronautical Journal*, Vol. 111, No. 1121, 2007, pp. 461–469.
- [45] Davison, P. M., *Development, Modelling and Control of a Multi-Degree-of-Freedom Dynamic Wind Tunnel Rig*, Ph.D. Thesis, Univ. of Bristol, 2003.
- [46] Grimm, G., Hatfield, J., Postlethwaite, I., Teel, A. R., Turner, M. C., and Zaccarian, L., “Antiwindup for Stable Linear Systems with Input Saturation: An LMI Based Synthesis,” *IEEE Transactions on Automatic Control*, Vol. 48, No. 9, 2003, pp. 1509–1525.  
doi:10.1109/TAC.2003.816965
- [47] Zheng, A., and Morari, M., “Anti-Windup Using Internal Model Control,” *International Journal of Control*, Vol. 60, No. 5, 1994, pp. 1015–1024.  
doi:10.1080/00207179408921506
- [48] Kapoor, N., and Daoutidis, P., “An Observer Based Anti-Windup Scheme for Nonlinear Systems with Input Constraints,” *International Journal of Control*, Vol. 72, No. 1, 1999, pp. 18–29.  
doi:10.1080/002071799221361
- [49] Khalil, H. K., *Nonlinear Systems*, Prentice-Hall, Upper Saddle River, NJ, 2002, pp. 102–103, 162, 163, 209, 539, 588.
- [50] Herrmann, G., Turner, M., Menon, P., Bates, D., and Postlethwaite, I., “Anti-Windup Synthesis for Nonlinear Dynamic Inversion Controllers,” *Proceedings of the IFAC ROCOND*, Toulouse, France, 2006, pp. 471–476.
- [51] Herrmann, G., Turner, M., and Postlethwaite, I., “Performance Oriented Anti-Windup for a Class of Neural Network Controlled Systems,” *IEEE Transactions on Neural Network*, Vol. 18, No. 2, 2007, pp. 449–465.  
doi:10.1109/TNN.2006.885037
- [52] Herrmann, G., Turner, M., and Postlethwaite, I., “Some New Results on Anti-Windup-Conditioning Using the Weston-Postlethwaite Approach,” *Proceedings of CDC*, Paradise Island, Bahamas, 2004, pp. 5047–5052.
- [53] Goldberg, D., *Genetic Algorithms in Search, Optimization and Machine Learning*, Addison Wesley Longman, Reading, MA, 1989, Chap. 3.